INL/CON-09-15519
PREPRINT

The Industrial Sodium Cooled Fast Reactor

ANFM 2009

Samuel E. Bays
Hongbin Zhang
Haihua Zhao

April 2009

The INL is a
U.S. Department of Energy
National Laboratory
operated by
Battelle Energy Alliance

Advances in Nuclear Fuel Management IV (ANFM 2009)
Hilton Head Island, South Carolina, USA, April 12-15, 2009, on CD-ROM, American Nuclear Society, LaGrange Park, IL (2009)

The Industrial Sodium Cooled Fast Reactor

Samuel E. Bays, Hongbin Zhang, Haihua Zhao
Idaho National Laboratory
P.O. Box 1625, MS 3870, Idaho Falls, ID 83403
Samuel.Bays@INL.gov, Hongbin.Zhang@INL.gov, Haihua.Zhao@INL.gov

Keywords: Sodium Fast Reactor, Enrichment Zoning, Molten Coolant Gas Cycle

ABSTRACT

This paper investigates the use of enrichment and moderator zoning methods for optimizing the r-z power distribution within sodium cooled fast reactors. These methods allow overall greater fuel utilization in the core resulting in more fuel being irradiated near the maximum allowed thermal power. The peak-to-average power density was held to 1.18. This core design, in conjunction with a multiple-reheat Brayton power conversion system, has merit for producing an industrial level of electrical output (2400 MWth, 1000 MWe) from a relatively compact core size. The total core radius, including reflectors and shields, was held to 1.78 m. Preliminary safety analysis suggests that positive reactivity insertion resulting from a leak between the sodium primary loop and helium power conversion system can be mitigated using simple gas-liquid centripetal separation strategies in the plant's primary loop.

1. INTRODUCTION

An attractive feature of the Sodium cooled Fast Reactor (SFR) is its high power density, allowing a high thermal rating for a small core size. However, despite the small size of the actual core, commercial SFRs power plants would still be subject to at best the same volume of plumbing required for safety, cooling and electricity production as that of Light Water Reactors (LWR). Additionally, a common safety feature for the widely used pool type design is to have a large sodium tank that allows a high thermal momentum for dampening transient response related to changes in sodium density. Even in modular SFR designs (~1000 MWth) the sodium tank, which also houses a sodium-to-sodium intermediate heat exchanger (IHX), can be of the same size scale as that of an LWR pressure vessel (~3400 MWth). This intermediate loop separates the activated sodium of the primary system with the power conversion system, typically a steam Rankine cycle. This separation eliminates the possibility of an energetic sodium reaction (i.e., sodium fire) between the sodium that is in contact with the core and the steam loop. In order for the SFR to truly be capital cost competitive with commercial LWRs, the extra volume of power plant occupied by these additional sodium systems must be minimized or replaced with a more space savings and cost efficient design strategy.

It is the IHX and primary sodium recirculation pumps that contribute to the added volume of the primary tank. The intermediate loop also adds additional plumbing and

cost to the SFR plant. All of this effort is made to deliver power to a steam Rankine cycle that limits the thermal efficiency to approximately 36-42%[1,2,3]. It has been proposed by Zhao et. al. that the Rankine cycle can be replaced by a multiple reheat molten coolant helium gas cycle (MCGC) to give a thermal efficiency of 42%[4,5,6]. This means that a thermal rating of 2400 MWt is required to yield 1000 MWe, as opposed to 2800 MWth for an efficiency of 36%. The MCGC could elliminate the intermediate loop and steam cycle with compact sodium-to-helium heaters providing power to a Brayton power cycle with multiple reheat, intercooling and recuperation (**Fig. 1**). The figure shows the advanced loop type SFR plant design by Zhao et. al.[6].

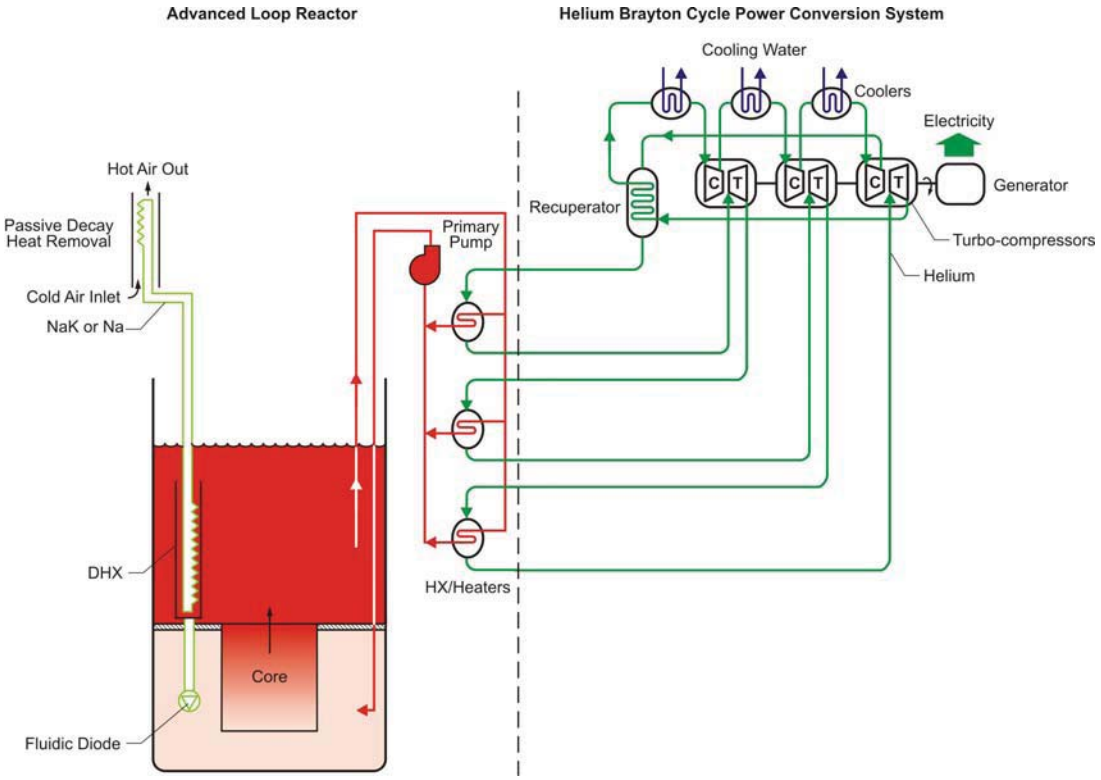

Fig. 1 An advanced loop type SFR with a multiple reheat helium Brayton cycle.

The choice of a loop-type as opposed to a pool-type design has the potential for primary tank size reduction benefit. Some volume is allocated to accommodate a Direct Reactor Auxiliary Cooling System (DRACS) Heat Exchanger (DHX), which is a passive decay heat removal system that is scalable to the volume of the primary tank[7]. Also, it should be noted that replacement of large steam generators with more compact Printed Circuit Heat Exchangers (PCHE) or Plate Fin Heat Exchangers (PFHE) for a sodium-to-helium heat transfer can result in a size reduction of the plant's sodium containing building.

The average thermal rating for a typical SFR is about 300 MWth/m^3. Assuming the core power density is this average everywhere, the minimum core volume for a 2800 MWth and a 2400 MWth rating is 9.3 m^3 and 8 m^3, respectively. Assuming a one meter core height, the minimum core radii for these two hypothetical designs are 1.72 m and 1.60 m, respectively. This difference is almost the width of one row of fuel. Therefore,

the higher thermal efficiency allows for a 14% reduction in the minimum core volume and a 7% reduction in core radius.

In reality, the power distribution in a SFR is not flatly distributed. Due to the long mean-free-path of fast energy neutrons, the buckling or curvature of the SFR flux and power profile is significant. The high flux gradient translates into a high neutron leakage at the core periphery. This leakage and associated power gradient can cause the fuel in the outer core to have a low power density compared to the inner core. Because of this large discrepancy in regional power sharing, the outer core can experience excess fuel performance margin and the inner core to be pressed to the fuel's design limit. This paper explores enrichment (i.e., TRU/HM by volume) and local spectrum moderation techniques that optimize the power profile to be virtually flat across the core, despite a high flux gradient. If more margin can be provided to the inner core region due to power flattening, it is conceivable that the average power density of the core could be increased. This equates into a decrease in core volume for constant thermal rating.

This level of power flattening is achieved by: 1.) axial and radial enrichment zoning 2.) slightly moderating the neutron flux near the reflector to locally increase fuel utilization and absorptions in fissile atoms. Moderation in the radial reflector is also advantageous from the standpoint of reactor vessel (RV) life. Using moderation with a neutron absorber in the radial reflector can reduce the number of rows of reflector assemblies needed to protect the RV from fast neutron damage. This paper investigates core design strategies relatively common to LWRs that when applied to SFRs reduce the wasted space associated with fast neutron leakage, thus fully realizing the space benefits of the SFR high specific power rating. The concept core design for exploring these optimizations is called the Industrial Sodium Cooled Fast Reactor (ISFR).

2. DESIGN AND METHODOLOGY

The ISFR core design philosophy is to deliver a power rating comparable to commercial LWRs but with an optimized compact core size. The resulting core design is assumed as the heat source for the helium Brayton power conversion system.

2.1 Description of Reactor Physics Tools

The fast reactor codes MC^2-2, DIF3D and REBUS were used for the reactor physics and fuel cycle calculations[7,9,10]. The MC^2-2 code was used to generate a 33 group cross section set for each driver fuel enrichment zone, the targets, reflectors and shields. Starting with an ultra fine group ENDF-V/B cross section library, MC^2-2 creates a collapsed cross section set by performing a zero dimensional critical buckling search using the extended P1 method[7]. Using this collapsed cross section set, the DIF3D diffusion code was used to solve the multi-group steady state neutron diffusion equation using a hexagonal-z nodal coordinate system[9]. In the nodal discretization, each hexagonal node in the lateral direction represents an assembly. REBUS uses DIF3D to perform a criticality search for the uncontrolled excess reactivity at each time step in its fuel depletion algorithm[10]. In this search, the fresh fuel transuranic enrichment is adjusted until the specified cycle length is achieved. For each enrichment adjustment, the fluxes from DIF3D are used to carry out the isotopic buildup/depletion process over the time of

the irradiation cycle. REBUS also performs the in-core fuel management and out of core cooling, reprocessing and re-fabrication calculations for each reactor cycle. These operations are carried out until the beginning of equilibrium cycle (BOEC) excess reactivity is found for the prescribed cycle length at equilibrium.

The sodium density and void worth calculations, presented in Section 4, were performed for the uncontrolled core state (control rods out). The total isotopic composition in each axial and radial region from the REBUS-3 output file was copied into a new DIF3D (no depletion) input file. The sodium density was then adjusted incrementally to generate the density worth curve. The void worth curves were generated by locally (i.e., one row of fuel assemblies at a time) or globally (all assemblies less than the specified row number) voiding all of the sodium from the region of interest. In these calculations, the sodium in the corresponding MC^2-2 calculation was also adjusted. The parametric adjustment of the sodium density and/or sodium void location was performed by the Multi-Reactor Design and Analysis Platform (MRDAP) being developed at Idaho National Laboratory.

2.2 Core Design Description

The core design for the ISFR will exhibit a high degree of core enrichment zoning for the purpose of achieving optimized power flattening in both radial and axial directions. This is unique from previous SFR core designs because enrichment zoning is typically only carried out in the radial direction[1]. Another design innovation of the ISFR is the introduction of zirconium-hydride dilution rods. **Fig. 2** gives the radial and axial profile of the ISFR.

The ISFR has four radial enrichment zones and five axial enrichment sub-zones for each radial region. The minimum and maximum enrichment in these zones are 23% and 57%, respectively. Here enrichment is defined as the TRU enrichment per HM by volume[*]. This high degree of enrichment splitting produces a nearly flat power profile in both radial and axial directions despite the large flux gradient. Because of this flat power distribution, all fuel is forced to perform at or near its peak power performance. Hence, the ISFR has virtually zero wasted space in terms of low power density regions on the core perimeter, as will be discussed in Section 3.

Another design innovation of the ISFR core design is the introduction of zirconium-hydride dilution rods. To decrease the spatial gradient of the neutron flux leaving the core, the amount of moderator in each radial enrichment zone is increased for increasing radius. The result is a decrease in the neutron mean free path for increasing radius. **Table 1** and **Table 2** provide a detailed description of the zirconium-hydride zoning and enrichment zoning, respectively. The slight moderation of the zirconium-hydride rods achieves two goals: (1) preferentially increase neutron capture in U-238 in the lowest uranium concentration (i.e., highest enrichment) zones (2) soften the fast flux such to allow for longer cladding and structural material lifetimes.

[*] The ISFR fuel is a metallic U/TRU/10-Zr fuel alloy. Therefore, the metal fuel "slug" is 10w/o by weight and approximately 20v/o by volume.

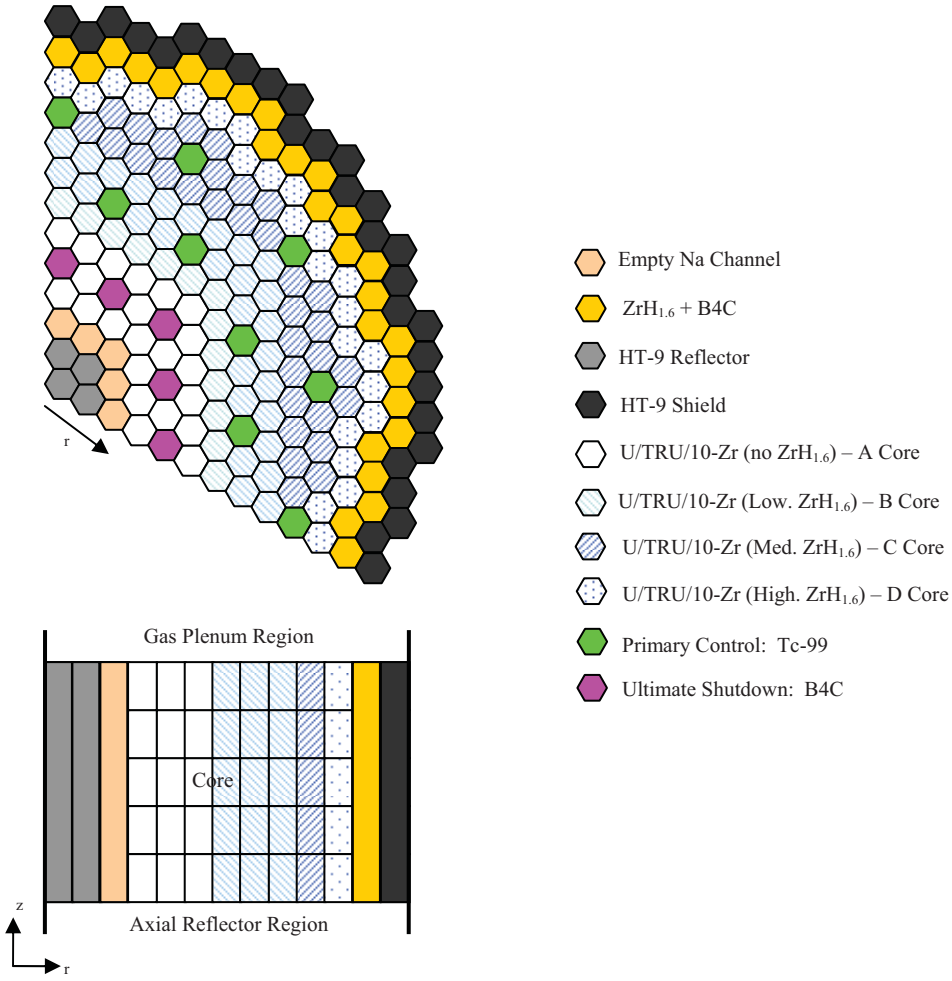

Fig. 2 ISFR radial core layout

Table 1 Moderating zone description.

	A Core "inner"	B	C	D Core "outer"
Total Pins	271	271	271	271
Fueled Pins	235	235	235	235
Na Filled Pins	36	30	24	0
$ZrH_{1.6}$ Pins	0	6	12	36

Table 2 Enrichment zone splitting factors (F)

	A Core "inner"	B Core	C Core	D Core "outer"
80-100 cm - Top	1.25	1.25	1.50	2.25
60-80 cm	1.12	1.00	1.25	1.75
40-60 cm	1.00	0.90	1.12	1.50
20-40 cm	1.12	1.00	1.25	1.75
0-20 cm - Bottom	1.25	1.25	1.50	2.25

Note: HM volume fraction in metal fuel is 80v/o with the remainder being Zr
$E_{region}=E_{feed}\times F$, $E_{feed}=25.5\%$ (by volume)

The ISFR fuel cycle is based on a closed fuel cycle circuit assuming spent SFR fuel is cooled and reprocessed on-site[11]. The transuranics consumed by fission are replaced each cycle by an external supply of TRU supplied from separated Spent Nuclear Fuel (SNF). The isotopic composition of this external fissile feed corresponds to a pressurized water reactor fuel assembly irradiated to 51 MWD/kg, cooled for five years pre-reprocessing and cooled for an additional two years post-reprocessing. All of the SNF and fast reactor generated minor actinides (MA) are assumed to be retained in the ISFR's closed fuel cycle. **Table 3** gives a breakdown of the core design and irradiation cycle features.

Table 3 Core and fuel cycle design

Core Thermal Power, MWth	2400
Thermodynamic Efficiency, %	42
Capacity Factor, %	88
Cycle length, days	322.5
Spent Fuel Cooling, days	297.33
Fuel Recycle/Fabrication, days	148.66
Core Radius, m	1.60
Core+Reflector Radius, m	1.78
Number of Assemblies	
Total	342
A Core	60
B Core	96
C Core	114
D Core	72
Number of Cycles	
A Core	4
B Core	4
C Core	5
D Core	8
TRU Consumption Rate, g/MWY	154
Average Fuel Burnup, MWD/kg	160

2.3 Fuel and Material Selection

The ISFR is a metal (U/TRU/10-Zr) fueled core design. Metal fuels are denser then oxide fuels, thus allowing for a higher specific power. The lack of oxygen from the fuel type allows for a harder neutron spectrum in the absence of moderator. The harder spectrum allows the non-fissile isotopes (e.g., U-238, Np-237, Am-241) to have a higher fissile worth. These isotopes have a fission threshold at 1 MeV. Thus, the harder fast spectrum gives a higher fission-to-capture ratio for these isotopes. This is also important for space saving because higher fissile worth equates into a higher material buckling, and hence a smaller critical radius. Metal fuels were the driver fuel of Experimental Breeder Reactor – II (EBR-II). Ternary U/Pu/10-Zr fuels testing had begun at EBR-II during the

Integral Fast Reactor (IFR) program but ended when the program was cancelled in 1994. At a discharge burnup of ~11 atom percent (~120 MWD/kg), U/Pu/10-Zr alloy test assemblies showed excellent performance during irradiation[12]. The main drawback to metal fuels is a lower melting point than oxide, despite a much higher thermal conductivity. However, this issue may not be as significant as with oxide fuels due to the fact that the melting point of the steel cladding material (~1500^{o}C) is significantly higher than that of the fuel (~1100^{o}C). **Table 4** compares SFR oxide and metal fuels.

Table 4 Comparison of metal and oxide fuels in SFR design

Metal	Oxide
• High thermal conductivity • Low melting point • High slug restructuring, gas release • Bond sodium to permeates slug during irradiation, increasing pellet thermal conductivity • Eutectic liquefaction can cause cladding wastage • Large axial expansion coefficient • Higher specific power • Faster neutron spectrum (smaller critical radius)	• Low thermal conductivity • High melting point • Same as metallic fuel • Oxide fuel is not sodium bonded and thermal conductivity decreases with irradiation • Oxide pellets experience significant swelling and cracking • Axial swelling not as significant • Lower specific power • Softer neutron spectrum (larger critical radius)

The cladding material selected for the ISFR is a SFR grade ferritic/martensitic high chromium steel, HT-9, tested at EBR-II and the Fast Flux Test Facility (FFTF). The number of irradiation cycles for each fuel type was adjusted to ensure that the each driver assembly came as close to but restricted to be below a fast fluence limit for HT-9, 4×10^{23} cm^{-2} (E>0.1 MeV), at all times[13]. Eutectic phase formation between SFR metal fuel and cladding is a type of failure mechanism that can occur in SFR metallic fuels. Eutectic liquefaction is a result of metallurgical interaction between actinides (and fission products), and the iron in the HT-9 cladding, which produces a low melting point phase[14]. For cladding integrity, it is important to ensure the peak inner cladding wall temperature to be below 650^{o}C[15].

The maximum enrichment in the ISFR (57%) is significantly higher than the U/Pu/10-Zr fuels tested at EBR-II (~20%). A higher enrichment of Pu in U-Pu-Zr fuels tends to decrease the melting temperature of the alloy. Previous authors have proposed a high increasing the zirconium fraction in the alloy to raise the melting point back to the U/20-Pu/10-Zr level. However, the addition of the zirconium removes uranium from the fuel which decreases Doppler feedback and the delayed neutron value of the fuel. In this paper, the zirconium concentration is left at 10 weight percent. It should be noted that the highest enrichments in the core occur at the core periphery where leakage is highest. In this location of the core, the value of a localized power excursion that could lead to fuel melt is lowest as will be discussed in the sodium coolant void worth section. The enrichment in the most reactive region (i.e., core mid-plane in the B-region) is only 23%.

Zirconium-hydride was selected as the moderator dilution pin material for its high thermal conductivity and melting temperature. A hydrogen-to-zirconium stoichiometric ratio of 1.6 was selected for zirconium-hydride's delta phase which retains composition for temperatures up to 1000°C[16].

2.4 Fuel Assembly Design

The assembly design of the ISFR is similar to that of previous designs such as the Advanced Burner Reactor (ABR)[17,18]. The hexagonal assembly contains 271 wire-wrapped pins contained in a hexagonal HT-9 shroud. The bottom 1 m of fuel pin is an HT-9 plug that comprises the bottom end of the fuel pin. Because the gas release in fast reactor fuels is high, a rule of thumb of approximately 1.5 times the fuel height (1 m) is adopted for the gas plenum (1.5 m). The gas plenum occupies the upper end of the fuel pin. **Table 5** gives a description of the ISFR fuel assembly design.

Table 5 Fuel assembly design

Fuel Type	Metal
Core conversion ratio	0.70
Total Pins per Assembly	271
Non-Fueled Pins	36
Assembly pitch, cm	16.142
Inter-assembly gap, cm	0.432
Duct outside flat-to-flat, cm	15.710
Duct material	HT-9
Duct thickness, cm	0.394
Pins per assembly	271
Spacer type	Wire wrap
Bond material in gap	Na
Plenum height, cm	150
Core height, cm	100
Axial reflector height, cm	100
Overall pin length, cm	350
Fuel smeared/ fabrication density, % TD	75/100
Pin outer diameter, cm	0.70
Cladding thickness, cm	0.06
Spacer wire wrap diameter, cm	0.0797
Pin pitch-to-diameter ratio	1.15
Volume Fractions	
Fuel	21.22
Bond	8.16
Coolant	44.52
Non-Fueled Space	3.25
Clad and Structural	22.85

3. MINIMIZING CORE SIZE

The combination of enrichment and moderator zoning allows the highest concentration of U-238 in the inner core where there is no moderator and the lowest concentration of U-238 in the outer core where the moderation is highest. This strategy allows the design to have the highest overall macroscopic cross section worth either through increase of U-238 atomic concentration or via increase in the U-238 microscopic cross section worth. Because neutrons are being slowed down to be captured by the fuel by means of the moderator strategy, optimized neutron investment in U-238 is achieved. This not only can enhance safety through enhanced resonance capture feedbacks but also enhance neutron economy and hence fuel utilization in the outer core high enrichment regions.

The moderator zoning (including that in the reflector) also ensures that the flux being leaked from the ISFR has been slowed down appreciably to the point where not as many rows of radial reflectors and shields are needed to protect the core vessel from exposure to fast neutrons. This fact adds to the ISFR compact core design concept by reducing the amount of space needed in the reactor vessel for non-fueled assemblies (i.e., shields and reflectors).

3.1 Flux Spectrum Zoning

The flux spectrum for each assembly type in the ISFR is shown in **Fig. 3**. An identical core design with all non-fueled pins filled with sodium (i.e., no moderator) is given as well.

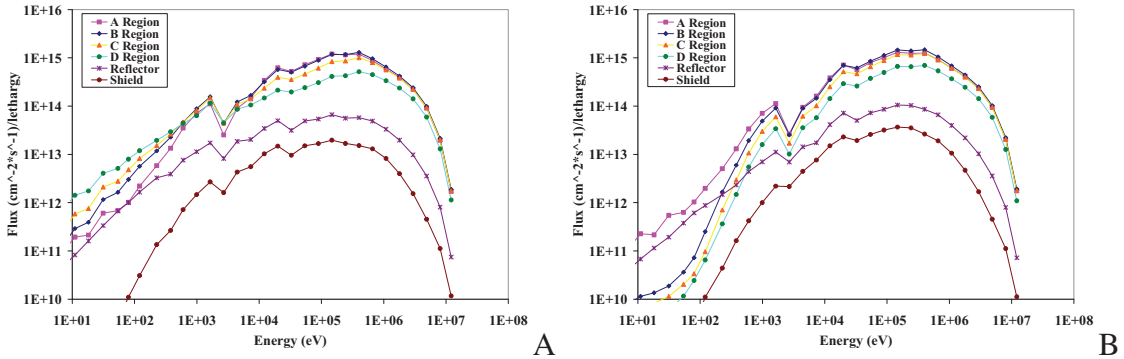

Fig. 3 Flux spectrum in a (A) moderated core and (B) non-moderated core

It is important to note that more of the flux exists at upper epithermal to lower fast spectrum range (i.e., below 1 keV) for increasing distance from the core center axis (**Fig. 3.A**). Therefore, even though the outer regions exhibit the smallest concentration of U-238 (i.e., smallest enrichment), it has the highest concentration of flux in the resonance energy region. For the non-moderated case (**Fig. 3.B**), the spectrum looks similar but with the flux falling off sharply below 1 keV. Note that the outermost enrichment zone, D Core, has the smallest flux at 1 MeV but the highest flux at E<1 keV. The increasing moderation with radius causes neutrons to slow down as they travel towards the core periphery. This causes the mean-free-path to decrease as more neutrons

are absorbed in the fuel. This increase in local fuel utilization in the core periphery causes neutron loss through leakage to go down and parasitic capture to go up. The decrease in leakage for the moderated case can be observed by comparing the flux distribution between the moderated and non-moderated cases (**Fig. 4**).

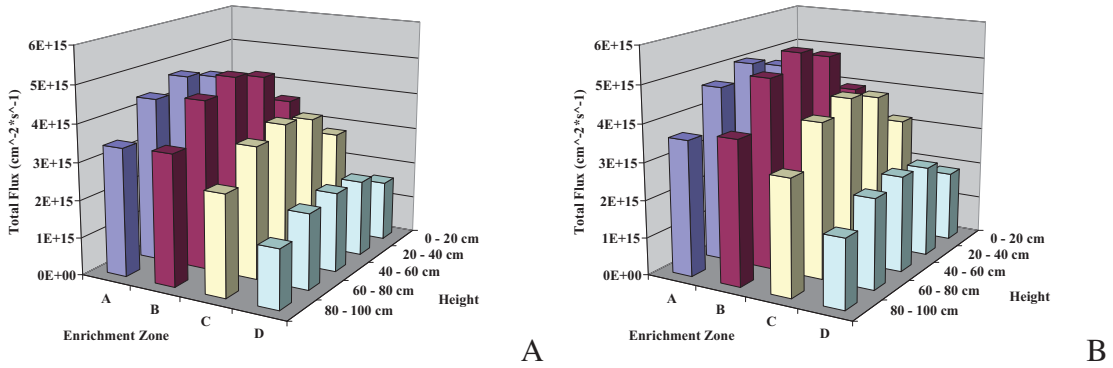

A B

Fig. 4 Flux distribution in a (A) moderated and (B) non-moderated core

Geometric buckling is defined as $-(d\Phi/dx)/\Phi$. Notice that the gradient ($d\Phi/dx$) of the flux does not change greatly between **Fig. 4.A** and **Fig. 4.B**. However, the magnitude (Φ) of the flux in the moderated case is less than that of the non-moderated case. The average fluxes are 3.37×10^{15} $cm^{-2}s^{-1}$ and 3.81×10^{15} $cm^{-2}s^{-1}$ for the moderated and non-moderated cases, respectively. Thus, the geometric buckling is slightly less in the moderated design.

3.2 Core Power Shape

The increase in fuel utilization can also be seen by observing the power distribution between the moderated and non-moderated cases (**Fig. 5**). The use of moderator allows the enrichment zoning in the core to be used more effectively than in the non-moderated case.

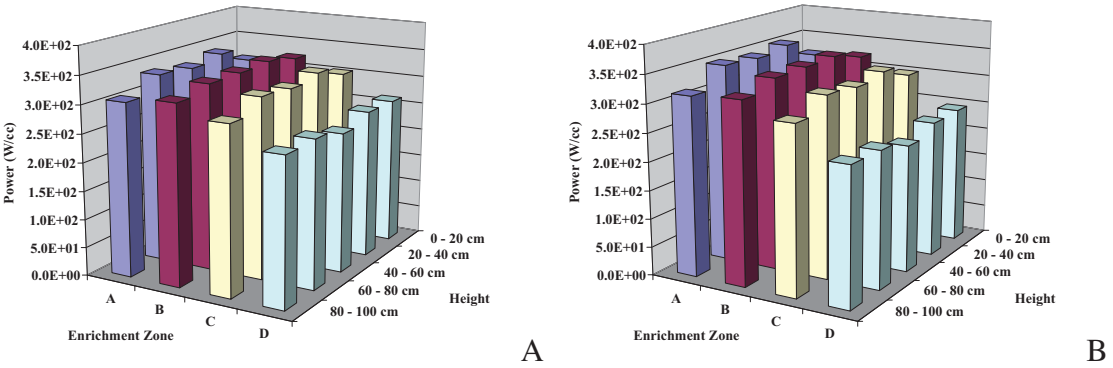

A B

Fig. 5 Power distribution in a (A) moderated and (B) non-moderated core

The combination of enrichment and moderator zoning gives a flattened power profile. The highest power density in the ISFR (moderated case) is 360 W/cm^3 which occurs in Row 9 (**Fig. 6**). The smallest power density is 250 W/cm^3 which occurs in the

outermost row of fuel (Row 11). The average power in the core is 306 W/cm^3. Thus, the maximum and minimum r-z regional power peak factors are 1.17 and 0.81, respectively.

The peak Linear Heat Generation Rate (LHGR) is 35 kW/m occurring at the axial mid-plane of the A-region at beginning-of-life (BOL). The average LHGR for the core is 29.5 kW/m. This gives an absolute space and time dependent peaking of 1.19. By comparison, the ABR's peak and average LHGR are 37.7 kW/m and 23.3 kW/m, respectively giving a peaking factor of 1.6[18]. The peak and average LHGR for Super-Phénix was 48kW/m and 30kW/m, respectively giving a peaking factor of 1.6[1].

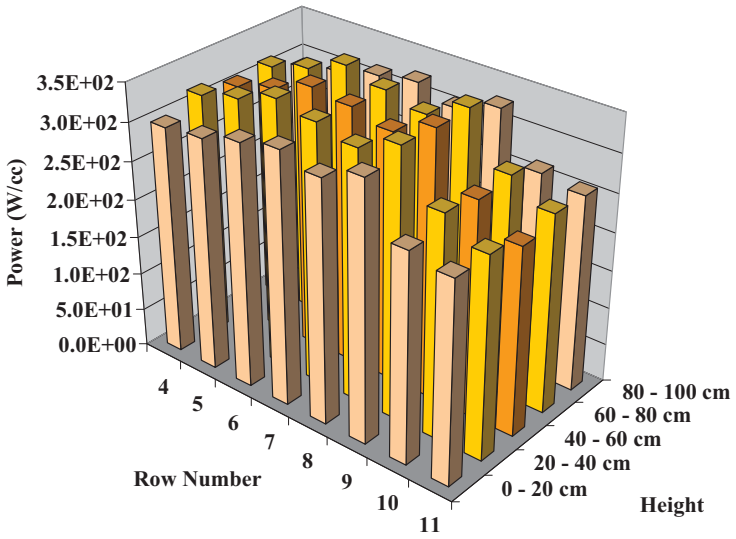

Fig. 6 ISFR power distribution by row number

4. CORE SAFETY ANALYSIS

The ISFR, like most SFR designs, has a positive sodium density coefficient. The positive reactivity feedback is a direct consequence of neutron energy spectrum hardening resulting from the loss of the slight neutron down-scattering and capture provided by the sodium coolant. When the spectrum hardens, the lack of down scattering causes the number of neutrons above the fission threshold of fertile isotopes (U-238 and MAs) to increase. An increase in above-threshold fissions causes an increase in the neutron multiplication contribution of these fertile isotopes.

The loss of sodium also influences the amount of neutron leakage from the core which increases as the down-scattering from sodium atoms decreases. The resulting effect of the spectrum hardening on core reactivity is dominated by the spatial dependence of this neutron leakage[19]. This spatial dependence is important for evaluating the void scenario most threatening to core safety. In the SFR plant system proposed by Zhao et. al., the low pressure sodium of the primary tank is separated by only a single heat exchange wall, not an entire intermediary sodium loop, from the high pressure helium of the power conversion system[6]. In this section, various levels of failure of this barrier and the associated reactivity feedbacks are evaluated.

4.1 Sodium Density Worth

For a change in sodium density, leakage is increased evenly across the entire core geometry. This is the case for many small helium bubbles being released evenly throughout the core from a small leak in the compact heat exchanger. Since a PCHE typically has flow channels at the order of mm, only mm scale break could happen with some credible chance[6]. It is expected that the resulting gas release from a 1 mm diameter break into the core would be evenly distributed throughout the primary tank sodium. This small leak would give a void fraction in the primary tank sodium on the order of 1%[6] . A 1 cm scale break should be extremely impossible for a well designed compact heat exchanger. For worst case scenario, a large 1 cm scale break will result in 20% to 30% maximal void fraction in the core[6]. For such a large break, it is suggested that a gas-liquid centripetal separator be placed down-flow of the IHX (i.e., PCHE or PFHE) to avoid this level of instantaneous gas insertion.

A large scale displacement of all the sodium in the core creates as much as a full percent of instantaneous positive reactivity insertion (**Fig. 7**). Such a situation is representative of bulk sodium boiling which is unlikely for systems with high thermal momentum, such as pool type designs or loop designs with primary pumps having long coast-down times. A change in sodium density of 30% would cause almost a full percent change in reactivity. Assuming a delayed neutron fraction typical of SFR's (~0.003), this would correspond to about $5.00 of reactivity insertion. However, as can be seen from **Fig. 7**, for a small decrease in sodium density, as a result of a small leak, the reactivity insertion may be manageable to within 0.3% or approximately $1.00.

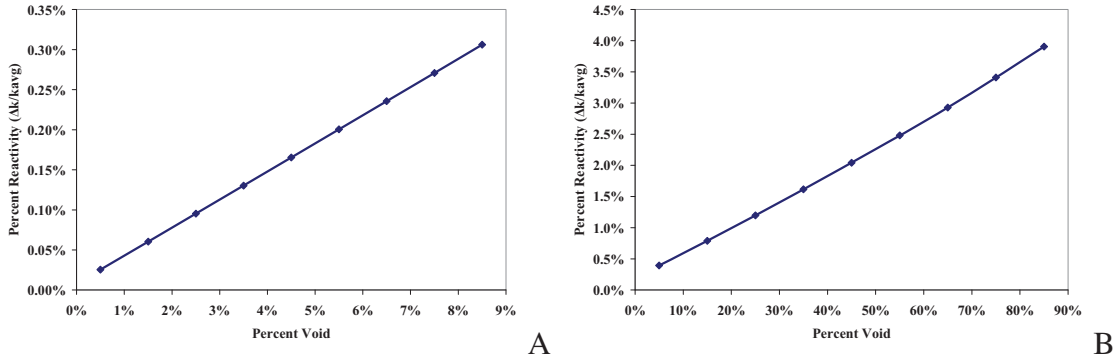

A B

Fig. 7 Sodium density worth curve for (A) 0-10% (B) 0-100% void fraction

4.2 Local and Global Sodium Void Worth

For a larger than 1 cm IHX break with a large bubble getting past the gas-liquid separator, it is conceivable that a bubble could enter the inlet nozzle of a single assembly, thus displacing the assembly's sodium and causing a *localized* void. This local void, if near the active core periphery, can cause reactivity to decrease by allowing leakage to increase. If placed away from the periphery, the localized leakage is not enough to offset the increase in multiplication from spectrum hardening, thus causing core reactivity to increase (**Fig. 8.A**). However, the positive reactivity insertion for any given assembly being voided is only a few tenths of a percent of reactivity per assembly

(Max.~$0.08/assembly in row seven). It is important to note that the highest sodium void worth occurs in the seventh row. This location has the smallest enrichment in the entire core (**Table 2**) and the highest U-238 concentration. Therefore, it is expected that this region will also have the largest resonance worth and Doppler feedback.

Finally, a large-scale failure of the heat exchanger could allow a very large bubble to enter the core, displacing the sodium in many or all assemblies. In this worst case scenario, the reactivity effect is due to a *globally* voided portion of the core. The amount of positive reactivity feedback steadily increases for global voids of increasing radius, starting at the center, until the outermost row of fuel is voided (**Fig. 8.B**) (Max.~$14.50 in row 10).

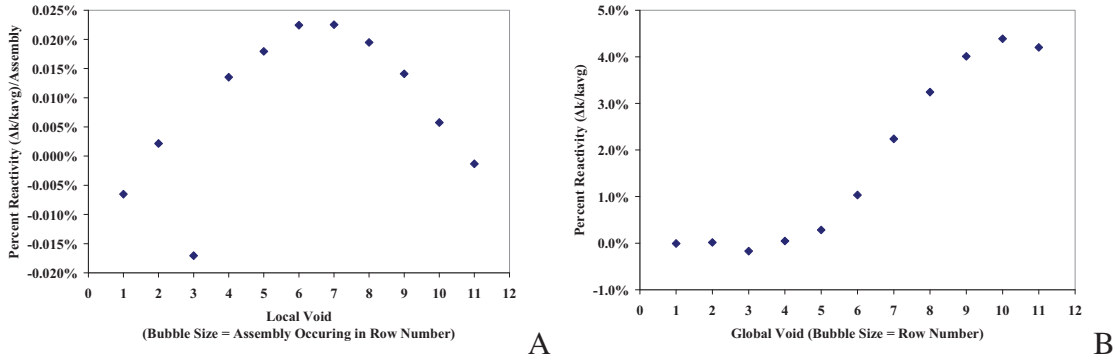

Fig. 8 Sodium void worth curves for (A) local void (B) global void insertion

However, it should be noted that because the ISFR is an annular core design, a large bubble inserted into the core center has zero to negative impact on core reactivity. In fact, the reactivity value of a large bubble insertion does not become significantly large until the entire inner enrichment zone "A" of the core has been voided (Row 4 – Row 6). This suggests that an annular core design can be made to be very resilient to a large size void insertion. This is particularly true if the mechanical design of the sodium inlet plenum is made to ensure the bubble enters the core radial center. An example of such a mechanical design feature would be introducing centrifugal rotation of the sodium at the inlet plenum below the lower grid plate.

4.3 Mechanical Feedback

Spectrum hardening can be unfavorable if there is no other competing feedback mechanism that can negate the void induced positive reactivity insertion. For SFRs, some negative reactivity feedback comes in the form of Doppler resonance broadening of capture cross sections as the fuel temperature increases. Additionally, because SFRs typically exhibit a high degree of leakage, they can rely on feedback mechanisms that increase leakage as the fuel and structural materials increase in temperature. The negative reactivity feedback caused by this fuel expansion is most pronounced in metallic fuels and was a key control feature of EBR-II[20].

The bowing of fuel assemblies in the radial direction is caused by lateral temperature gradients across the cross-sectional area of the fuel assembly[21]. Axial expansion is caused by fuel elongation as a result of thermal expansion coefficients of the

fuel slug[22]. Axial expansion of metal fuel is more pronounced than for oxide fuels due to the swelling brought on by thermal expansion of coalesced fission gas voids in metallic fuel matrix which becomes highly malleable at the elevated temperatures of a transient[22]. This quantification of these feedback mechanisms on the ISFR safety design is left for future work.

5. CONCLUSIONS

Optimization based on enrichment and spectrum zoning can bring significant improvements to the peak power margin within a SFR. Using a small number of zirconium-hydride pins per assembly, the amount of moderating pins was increased with increasing radius. The increase in moderator with increasing radius causes a decrease in geometric buckling and increase in fuel utilization. This allowed more neutrons to be invested in fuel atoms in the outer two rows of fuel as opposed to being leaked through them to the outer reflector. The increase in fuel utilization at the core periphery allowed for a higher power density than without moderation. Using this spectral zoning strategy with both radial and axial enrichment zoning, gave a virtually flat r-z power profile. This flat power profile ensures that the peak power factor is only 1.18 compared to a value of at least 1.5 for traditional core designs. The large margin enables the designed average core power density to be high without endangering fuel integrity. This fact in conjunction with a high thermal efficiency, due to the multiple reheat helium Brayton power conversion system, makes possible an industrial scale electrical output of 1000 MWe, without requiring a primary system larger than that of commercial light water reactors. The ISFR core radius, including reflector and shields, is 1.78 m.

The replacement of the traditional SFR's intermediate sodium loop and steam Rankine cycle with a helium Brayton cycle could potentially decrease the cost of industrial SFRs. The removal of water from the SFR power plant design greatly reduces the likelihood of sodium fire. However, this option adds another degree of complexity to the SFR's safety case. Four types of reactivity insertions based on inert helium gas displacing sodium within the core were investigated.

- First, the most credible helium insertion would be a small millimeter sized leak in the sodium-to-helium IHX. This kind of leak would most likely distribute helium evenly throughout the primary system, thus decreasing sodium density on the order of 1% amounting to a reactivity insertion of about \$1.

- Second, a less likely 1 cm diameter leak would cause a bulk sodium density change of 20-30% resulting in a \$5 reactivity insertion. It is recommended that a gas-liquid centripetal separator downstream of the IHX is necessary to mitigate the likelihood of this scenario.

- Third, a local void displacing the sodium within a single fuel assembly was evaluated. This type of void does not insert much more than 10¢ per assembly.

- Finally, a large global void where a large helium bubble displaces much of the helium in the core was investigated. Due to the annular core design, it was found that the first six rows of assemblies could be voided before significant reactivity

insertion begins. This includes the entire inner reflector and the first three rows of fuel. It is suggested that a second centripetal scheme be employed to allow centrifugal rotation of the sodium at the inlet plenum below the lower grid plate to ensure that a large global void displaces sodium from the inner core first.

NOMENCLATURE

ABR	Advanced Burner Reactor
BOEC	Beginning of Equilibrium Cycle
BOL	Beginning of Life
DHX	DRACS Heat Exchanger
DRACS	Direct Reactor Auxiliary Cooling System
EBR-II	Experimental Breeder Reactor - II
Enrichment	Volumetric ratio of TRU per HM
EOEC	End of Equilibrium Cycle
EOL	End of Life
FFTF	Fast Flux Test Facility
HM	Heavy Metal
IFR	Integral Fast Reactor
IHX	Intermediate Heat Exchanger
ISFR	Industrial Sodium cooled Fast Reactor
LWR	Light Water Reactor
LHGR	Linear Heat Generation Rate
MA	Minor Actinide
MCGC	Molten Coolant helium Gas Cycle
MRDAP	Multi-Reactor Design and Analysis Platform
PCHE	Printed Circuit Heat Exchanger
PFHE	Plate Fin Heat Exchanger
RV	Reactor Vessel
SFR	Sodium cooled Fast Reactor
SNF	Spent Nuclear Fuel
TRU	Transuranic

ACKNOWLEDGMENTS

The authors would like to thank Josh Cogliati, Michael Milvich and Prashant Jain for their efforts developing the MRDAP software suite.

This paper was prepared for the U.S. Department of Energy Office of Nuclear Energy, Science, and Technology under DOE Idaho Operations Office Contract DE-AC07-05ID14517.

REFERENCES

1. IAEA, Fast Reactor Database – 2006 Update, IAEA-TECDOC-1531, (2006).

2. E. GLUEKLER, “U.S. Advanced Liquid Metal Reactor (ALMR),” *Progress in Nuclear Energy*, **31**, 1, pp. 43-61 (1997).

3. J. LEFEVRE, C. MITCHEL, G. HUBERT, "European Fast Reactor Design", *Nuclear Engineering and Design*, **162**, pp. 133-143 (1996).

4. H. ZHAO, P. PETERSON, "Optimization of Advanced High-Temperature Brayton Cycles with Multiple Reheat Stages," *Nuclear Technology*, **158**, pp. 145-157 (2007).

5. H. ZHAO, H. ZHANG, V. MOUSSEAU, P. PETERSON, "Improving SFR Economics through Innovations from Thermal Design and Analysis Aspects," *Nuclear Engineering and Design*, (2009), doi:10.1016/j.nucengdes.2009.02.012.

6. H. ZHAO, H. Zhang, S. Bays, "Use of Multiple Reheat Helium Brayton Cycles to Eliminate the Intermediate Heat Transfer Loop for Advanced Loop Type SFRs," *Proc. of ICAPP'09 – Nuclear Energy – Winning a Sustainable Future*, Tokyo, Japan, May 10-14, 2009 (2009).

7. H. ZHANG, H. ZHAO, V. MOUSSEAU, R. SZILARD, "Design Considerations for Economically Competitive Sodium Cooled Fast Reactors," *Proc. of ICAPP'09 – Nuclear Energy – Winning a Sustainable Future*, Tokyo, Japan, May 10-14, 2009 (2009).

8. H. HENRYSON, B. TOPPEL, C. STENBERG, "MC^2-2: A Code to Calculate Fast Neutron, Spectra and Multi Group Cross Sections," ANL-8144, (1976).

9. K. DERSTINE, DIF3D: "A Code to Solve One, Two, and Three Dimensional Finite Difference Diffusion Theory Problems," ANL-82-64, (1984).

10. B. TOPPEL, "A User's Guide to the REBUS-3 Fuel Cycle Analysis Capability," ANL-83-2, (1983).

11. D. WADE and R. HILL, "The Design Rationale of the IFR," *Progress in Nuclear Energy*, Vol. 31, No. 1, pp. 13-42 (1997).

12. H. TSAI, A. COHEN, M. BILLONE, and L. NEIMARK, "Irradiation Performance of U-Pu-Zr Metal Fuels for Liquid Metal Cooled Reactors," *Proc. of ICONE3*, April 23-27, 1995, Kyoto, Japan, (1995).

13. D. GELLES, "Microstructural Development in Reduced Activation Ferritic Alloys Irradiated to 200 dpa at 420C," *Journal of Nuclear Materials*, **212-215**, pp. 714-719 (1994).

14. G. HOFMAN, L. WALTERS, and T. BAUER, "Metallic Fast Reactor Fuels," *Progress in Nuclear Energy*, **31**, 1-2, pp. 83-110 (1997).

15. R. PAHL, C. LAHM, S. HAYES, Performance of HT9 Clad Metallic Fuel at High Temperature, *Journal of Nuclear Materials*, **204**, pp. 141-147 (1993).

16. K. MOORE and W. YOUNG, "Phase Studies of the Zr-H System at High Hydrogen Concentrations," *Journal of Nuclear Materials*, **27**, pp. 316-324 (1968).

17. E. HOFFMAN, W. YANG, R. HILL, "Preliminary Core Design Studies for the Advanced Burner Reactor over a Wide Range of Conversion Ratios," ANL-AFCI-177 (2006).

18. T. KIM and W. YANG, "A Metal Fuel Core Concept for 1000 MWt Advanced Burner Reactor (Interim Report)," ANL-AFCI-185,rev1 (2007).

19. K. WIRTZ, *Lectures on Fast Reactors*, American Nuclear Society, p. 133, La Grange Park, Illinoise, (1982).

20. H. PLANCHON, R. SINGER, D. MOHR, and E. FELDMAN, "The Experimental Breeder Reactor II Inherent Shutdown and Heat Removal Tests - Results and Analysis," *Nuclear Engineering and Design*, **91**, pp. 287-296, (1986).

21. H. OIGAWA, S. IIJIMA, and M. BANDO, "Experiments and Analysis on Fuel Expansion and Bowing Reactivity Worth in Mock-up Cores of Metallic Fueld Fast Reactors at FCA," *Journal of Nuclear Science and Technology*, **36**, 10, 902-913 (1999).

22. E. RHODES, T. BAUER, G. STANFORD, J. REGIS, and C. DICKERMAN, "Fuel Motion in Overpower Tests of Metallic Integral Fast Reactor Fuel," *Nuclear Technology*, **98**, pp. 91-99 (1992).